LETTERS

NUMB controls p53 tumour suppressor activity

Ivan N. Colaluca[1,2], Daniela Tosoni[1,2], Paolo Nuciforo[1], Francesca Senic-Matuglia[1], Viviana Galimberti[2], Giuseppe Viale[2,3], Salvatore Pece[1,2,3] & Pier Paolo Di Fiore[1,2,3]

NUMB is a cell fate determinant, which, by asymmetrically partitioning at mitosis, controls cell fate choices by antagonising the activity of the plasma membrane receptor of the NOTCH family[1]. NUMB is also an endocytic protein[2], and the NOTCH–NUMB counteraction has been linked to this function[3,4]. There might be, however, additional functions of NUMB, as witnessed by its proposed role as a tumour suppressor in breast cancer[5]. Here we describe a previously unknown function for human NUMB as a regulator of tumour protein p53 (also known as TP53). NUMB enters in a tricomplex with p53 and the E3 ubiquitin ligase HDM2 (also known as MDM2), thereby preventing ubiquitination and degradation of p53. This results in increased p53 protein levels and activity, and in regulation of p53-dependent phenotypes. In breast cancers there is frequent loss of NUMB expression[5]. We show that, in primary breast tumour cells, this event causes decreased p53 levels and increased chemoresistance. In breast cancers, loss of NUMB expression causes increased activity of the receptor NOTCH[5]. Thus, in these cancers, a single event—loss of NUMB expression—determines activation of an oncogene (NOTCH) and attenuation of the p53 tumour suppressor pathway. Biologically, this results in an aggressive tumour phenotype, as witnessed by findings that NUMB-defective breast tumours display poor prognosis. Our results uncover a previously unknown tumour suppressor circuitry.

p53 is one of the major tumour suppressor proteins[6]. Mutations in the *p53* gene are detected in ~50% of human cancers[7]. Indirect mechanisms also lead to p53 inactivation. HDM2 binds to p53 and hinders its transcriptional activity[8]. In addition, HDM2 regulates p53 half-life through its E3 ubiquitin-ligase activity[9,10]. The tumour suppressor ARF (alternative reading frame, and encoded by the *INK4a/ARF* locus; *INK4a* is also called *CDKN2A*) binds to HDM2 and interferes with its activity, thereby stabilizing p53 (ref. 11). Thus, in human tumours, amplification of the *HDM2* gene[12] or loss of the ARF protein[13] result in defective p53 activity. In breast tumours, p53 mutations and amplification of *HDM2* are not as frequent as in other tumours, being detected in ~20% and <10% of cases, respectively[14–16]. Similarly, homozygous deletions or mutations of the *INK4a/ARF* locus are rare[17–19]. Although epigenetic mechanisms might contribute to altered expression of HDM2 or ARF[18], other unknown circuitries of regulation of p53 might be subverted in breast tumours. NUMB is a candidate for this role, in that it binds to HDM2 (ref. 20) and is frequently underexpressed in breast cancers[5].

Previous work has shown interaction *in vivo* between overexpressed NUMB and HDM2 (ref. 20). Also the two endogenous proteins can be co-immunoprecipitated from cellular lysates of normal mammary MCF10A cells (Fig. 1a). In addition, the four described isoforms of NUMB all interact with HDM2 (Supplementary Fig. 1a). NUMB also co-immunoprecipitates with p53 (Fig. 1a). This is compatible with the existence *in vivo* of multiple binary complexes (NUMB–HDM2, NUMB–p53 and HDM2–p53), or of a tricomplex NUMB–HDM2–p53. In *in vitro* binding assays with purified proteins, all three binary complexes could form, indicating direct interactions between the three proteins (Supplementary Fig. 1b). The presence of nutlin, which inhibits the HDM2–p53 interaction[21], prevented the formation of the HDM2–p53 complex, but not of the HDM2–NUMB or p53–NUMB complexes (Fig. 1b). Thus, the NUMB–p53 and NUMB–HDM2 surfaces of interaction are distinct, at least in part, from that of the HDM2–p53 interaction. This pointed to the possibility of formation of a tricomplex *in vivo* (which might coexist with the various binary complexes)—a possibility confirmed by sequential immunoprecipitation experiments with endogenous (Fig. 1c) or overexpressed (Supplementary Fig. 1c) proteins. Nutlin and cisplatin strongly decreased the NUMB–HDM2, but not the NUMB–p53, interaction (Supplementary Fig. 1d, e). These results argue that the stability of the tricomplex is affected by agents disrupting the HDM2–p53 interaction and that it is regulated in response to stress signals.

We analysed the effects of *NUMB* knockdown (*NUMB*-KD) on p53 by targeting two different sequences in *NUMB* using short interfering RNA (siRNA) or short hairpin RNA (shRNA), respectively. Both methods yielded 80–90% decrease in NUMB levels and an approximately twofold decrease in the p53 steady-state levels (Fig. 1d and Supplementary Fig. 2a). This effect was NUMB-specific because ablation of the related protein NUMBL (NUMB-like) did not affect p53 levels (Fig. 1d). Importantly, approximately threefold-higher doses of genotoxic drugs (Fig. 1e, f and Supplementary Fig. 2b) were needed to induce, in knockdown cells, levels of p53 comparable to those induced in wild-type cells. Similar results were obtained in primary normal human mammary cells (Supplementary Fig. 2c). The reduced levels of p53 on cisplatin treatment were paralleled by a reduction in the levels of Ser 15-phosphorylated p53 (Fig. 1f), a marker of the activation status of p53. Furthermore, we observed marked reductions in the expression of several p53 transcriptional targets (Fig. 1f, g). Thus, in *NUMB*-KD cells, the overall activation status of p53 after DNA damage is reduced.

In *NUMB*-KD cells, *p53* messenger RNA levels were not altered (Fig. 2a), arguing for NUMB-mediated regulation of p53 at the post-transcriptional level. Indeed, the half-life of p53 was reduced in *NUMB*-KD versus control cells, from ~60 to ~20 min (Fig. 2b, c). The half-life of HDM2 was not affected, arguing that *NUMB*-KD does not primarily affect HDM2 stability (Fig. 2b, c).

The simultaneous silencing of *NUMB* and *HDM2* restored p53 to levels indistinguishable from that of control cells or *HDM2*-KD cells (Fig. 2d). Nutlin stabilizes and activates p53 (ref. 21). Nutlin treatment of MCF10A cells resulted in increased steady-state levels of p53 and of HDM2 (Fig. 2e), which confirms that the accumulated p53 protein is transcriptionally active. More importantly, nutlin reversed the effects of *NUMB*-silencing on p53 levels (Fig. 2e). Thus, there is a requirement for HDM2 in the regulation of p53 by NUMB.

[1]IFOM, the FIRC Institute for Molecular Oncology Foundation, Via Adamello 16, 20139, Milan, Italy. [2]European Institute of Oncology, Via Ripamonti 435, 20141 Milan, Italy. [3]Dipartimento di Medicina, Chirurgia ed Odontoiatria, Università degli Studi di Milano, 20122 Milan, Italy.

HDM2 regulates p53 turnover through its E3 activity. In *NUMB*-KD cells, we detected enhanced ubiquitination of p53, which was inhibited by nutlin (Fig. 2f), arguing for a direct counteraction of NUMB over the p53-ubiquitinating activity of HDM2. This was confirmed in *in vitro* assays in which glutathione *S*-transferase (GST)–p53 was used as a substrate for the E3 activity of HDM2. Under these conditions, ubiquitinated p53 was readily detectable (Fig. 2g). However, this effect was abolished in the presence of purified NUMB or nutlin (Fig. 2g; see Supplementary Fig. 3 for possible models for action of NUMB).

NUMB inhibits NOTCH activity. Thus, it was important to prove that the observed effects were not a consequence of deregulated NOTCH activity. We treated *NUMB*-KD cells with inhibitors of presenilin/γ-secretase (known as γ-secretase inhibitors, GSI) to abolish NOTCH activity. GSI had no significant effect on p53 levels in *NUMB*-KD or control cells (Fig. 2h and Supplementary Fig. 4a), ruling out participation of NOTCH to the observed NUMB regulation of p53. This was confirmed using gain-of-function mutants of NOTCH (Supplementary Fig. 4b).

We tested whether the NUMB–HDM2 counteraction was relevant to p53-dependent transcriptional activity. HDM2 significantly inhibited the trans-activating ability of p53 on a luciferase reporter gene. However, NUMB restored, albeit not completely, this ability in a dose-dependent fashion (Fig. 2i).

Perturbation of NUMB levels should result in alterations in p53-mediated responses to DNA damage. To monitor DNA damage, we analysed the levels of phosphorylation at serine 139 of histone H2AFX (γ-H2AX) in cells treated with cisplatin, because prolonged persistence of γ-H2AX is considered to be a marker of persistent DNA damage[22,23]. MCF10A cells were treated and then washed free of the drug and monitored for up to 48 h. In both *p53*-KD (Fig. 3a) and *NUMB*-KD (Fig. 3b, c) cells, we detected higher levels of γ-H2AX than in control cells, and demonstrated persistence of γ-H2AX during the cisplatin chase.

We also tested the effects of *NUMB* or *p53* ablation on perturbations of the cell cycle induced by genotoxic drugs. In MCF10A cells, cisplatin induced an S-phase block; this was, however, independent of p53 or NUMB, and thus not informative for our purposes (Fig. 3d and Supplementary Fig. 5). However, doxorubicin and SN38 induced a G2/M block and an S-phase block, respectively, which were partially rescued by *NUMB*-KD or *p53*-KD (Fig. 3d). This effect is better illustrated by correcting for the initial percentage of cells in the various phases of the cycle (Fig. 3d, right-most panel), because the ablation of NUMB or p53 caused some alterations in the cell cycle already at steady state.

After treatment and washout with doxorubicin or SN38, MCF10A cells did not efficiently re-enter the cell cycle for at least 20 h (Fig. 3e), probably owing to checkpoint activation. Conversely, *NUMB*-KD cells and *p53*-KD cells displayed accelerated exit from the blocked phase (Fig. 3e). Moreover, doxorubicin and SN38 caused a marked block of cell proliferation, which was partly alleviated by the silencing of *NUMB* or *p53*. In addition, even after washout of the drugs, the proliferation rate was more sustained in *NUMB*-KD and *p53*-KD cells compared to control MCF10A cells (Fig. 3f).

We then performed experiments under conditions of NUMB overexpression. Expression of NUMB–GFP (green fluorescent protein) in MCF10A cells increased the levels of p53 in both unstressed cells and cisplatin- or doxorubicin-treated cells (Supplementary Fig. 6a, b). The moderate, albeit reproducible, increase in p53 possibly reflects the fact that proliferating cells can tolerate only limited amounts of

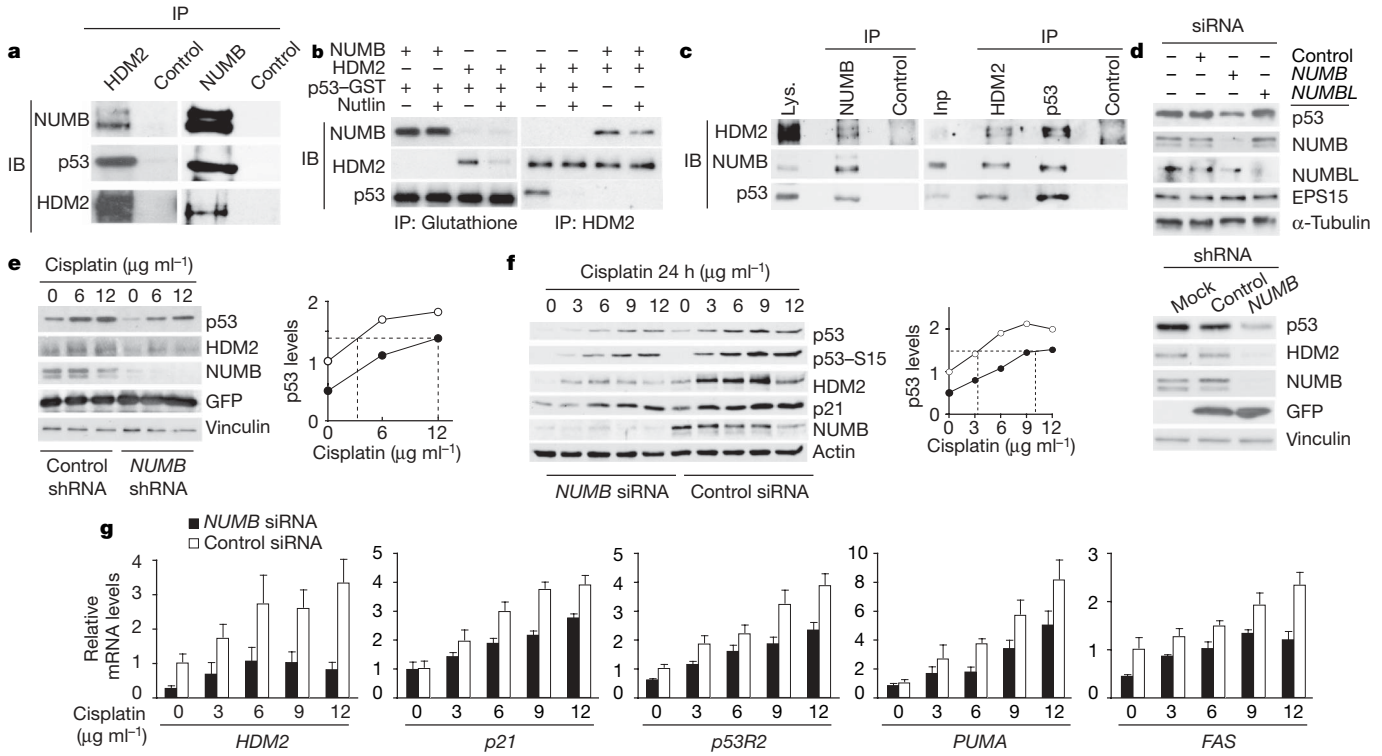

Figure 1 | NUMB interacts with and regulates p53. **a**, MCF10A lysates (3 mg) were immunoprecipitated (IP) and immunoblotted (IB). The control was an irrelevant antibody. **b**, Pure HDM2, GST–p53 and NUMB were mixed (3.2 nM each) and the solution was immunoprecipitated and immunoblotted as shown. **c**, Left, lysates (40 mg) from U2OS cells were immunoprecipitated with anti-NUMB (control, irrelevant antibody) and an aliquot (one-twenty-fifth) of the immunoprecipitate and immunoblot as shown. Right, the immunoprecipitate was eluted with the immunogenic NUMB peptide (amino acids 537–551); the immunoprecipitate and immunoblot were as indicated. Inp, one-fortieth of the eluate; Lys., lysate. **d**, MCF10A lysates, transfected as shown, were immunoblotted as indicated. **e**, **f**, MCF10A cells, transfected as shown, were exposed to cisplatin (24 h). The immunoblot was as indicated. Right, quantification (mean of three experiments) of p53 induction in control (open circles) and *NUMB*-KD cells (filled circles). **g**, Quantitative PCR with reverse transcription (RT–PCR) in control siRNA (open bars) and *NUMB*-KD (filled bars) MCF10A cells. Values represent mean (control siRNA/no cisplatin = 1) ± s.d. from two experiments. Cisplatin, 8 h.

p53. NUMB overexpression also enhanced p53-dependent transcriptional activity, and prolonged p53 half-life (from ~60 to ~120 min) (Supplementary Fig. 6a–d).

The above results demonstrate that NUMB overexpression increases p53 stability and activity, predicting enhancement of p53-mediated responses to genotoxicity, such as apoptosis. Thus, we monitored activation of caspases[24]. NUMB–GFP-transfected MCF10A cells displayed an approximately threefold-higher level of activated caspase-3 compared to control cells in response to cisplatin-induced DNA damage—an effect that was abolished by silencing of *p53* (Supplementary Fig. 6e, f). These results show that NUMB levels are relevant to the p53-mediated cellular responses.

In breast tumours, loss of NUMB expression is frequently detected[5]. These tumours should harbour reduced p53 levels and impaired p53-mediated responses. We addressed these issues in primary human breast tumour cells. These cells[5] can be cultivated from tumours displaying low or absent levels of NUMB (class 1 tumour cells) or normal levels of NUMB (class 3). We selected eight primary cultures (four of each for class 1 and class 3). The p53 coding sequence was normal in all selected primary cells (not shown).

In class 1 compared with class 3 cells, the steady-state levels of p53 were reduced (Fig. 4a) owing to increased proteasomal degradation, as shown by comparable *p53* mRNA levels in class 1 and 3 (Fig. 4b), and to restoration of p53 in class 1 cells by the proteasome inhibitor MG132 (Fig. 4a). The reduction in p53 levels was caused by loss of NUMB, by means of HDM2. Indeed, forced re-expression of NUMB–GFP (Fig. 4c) or silencing of *HDM2* (Fig. 4d) restored normal p53 levels in class 1, whereas it had a limited effect, as expected, in class 3 cells.

Deficient p53 activity is associated with resistance to the cytotoxic effects of chemotherapy[25]. Thus, NUMB-defective breast tumours should show resistance to genotoxic anticancer drugs. Indeed, class 1 cells exhibited higher resistance to cisplatin than class 3 cells (Fig. 4e). Re-expression of NUMB in class 1 cells restored responsiveness to cisplatin to levels comparable to those of control class 3 cells (Fig. 4e). NUMB-silencing in class 3 cells increased resistance to the drug to levels comparable to those of control class 1 cells (Fig. 4e). Nutlin restored the susceptibility of class 1 cells to cisplatin (Fig. 4e), and reverted the effects of NUMB ablation in class 3 cells (Fig. 4e), again implicating the HDM2–p53 circuitry.

Finally, we analysed a cohort of 443 breast cancer patients who received adjuvant chemotherapy. We found that NUMB status was inversely correlated with the major clinical and pathological parameters indicative of biologically aggressive neoplastic disease (Supplementary Table 1), and that it behaved as an independent predictor of poor prognosis (Fig. 4f). In conclusion, in breast tumours there is frequent loss of NUMB expression[5], and this event causes decreased p53 activity. Moreover, loss of NUMB expression is associated with poor prognosis, further arguing its clinical relevance. We note that lack of NUMB also leads to increased NOTCH activity[5]. Thus, the alteration of NUMB concomitantly leads to the activation of an oncogene, NOTCH, and to the attenuation of a tumour suppressor, p53.

Many questions await answers. It remains to be established where NUMB, HDM2 and p53 interact. This is not trivial because HDM2 and p53 are by-and-large nuclear proteins whereas NUMB is in the cytoplasm, mostly associated to biomembranes[2]. Similarly, our findings ask whether endocytosis participates to the regulation of p53, because NUMB is an endocytic protein. Of note, it has been shown

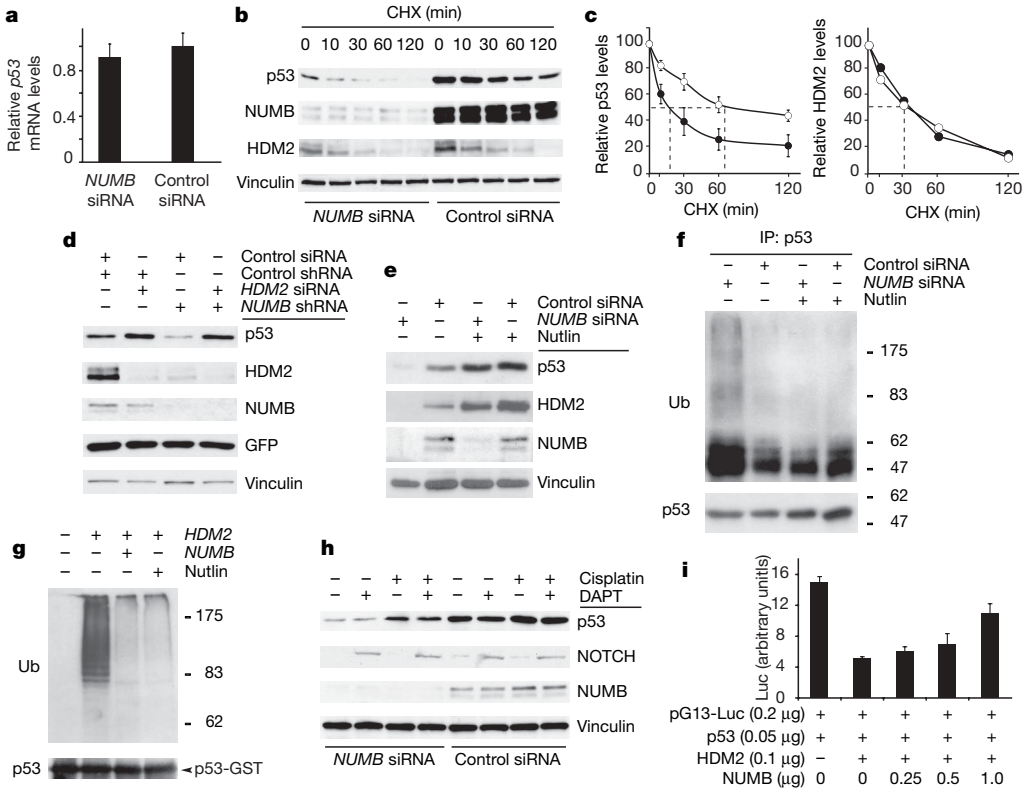

Figure 2 | NUMB regulates HDM2-mediated degradation of p53. **a**, *p53* mRNA levels in control-siRNA and *NUMB*-siRNA MCF10A cells. Values represent the mean ± s.d. (control siRNA = 1) from two experiments. **b**, **c**, MCF10A cells, transfected as shown, were treated with cycloheximide (CHX). Immunoblot was as indicated. In **c**, quantification of p53 and HDM2 levels in control-siRNA (open circles) and *NUMB*-siRNA (filled circles) cells are shown; values are expressed relative to time 0 (normalized to vinculin), and represent, in the case of p53, the mean ± s.d. of three experiments. **d**, **e**, **f**, Lysates from MCF10A cells, transfected and treated as indicated, were immunoprecipitated and immunoblotted as shown. In **f**, p53 levels were normalized by loading proportionally different amounts of cell extracts. **g**, GST–p53 was subjected to *in vitro* ubiquitination assay as indicated. Detection was in the immunoblot (Ub, anti-ubiquitin antibody). **h**, Lysates from MCF10A cells, transfected and treated as shown, were immunoblotted as indicated. **i**, Luciferase assay in U2OS cells transfected as indicated. Results represent mean ± s.d. from three experiments.

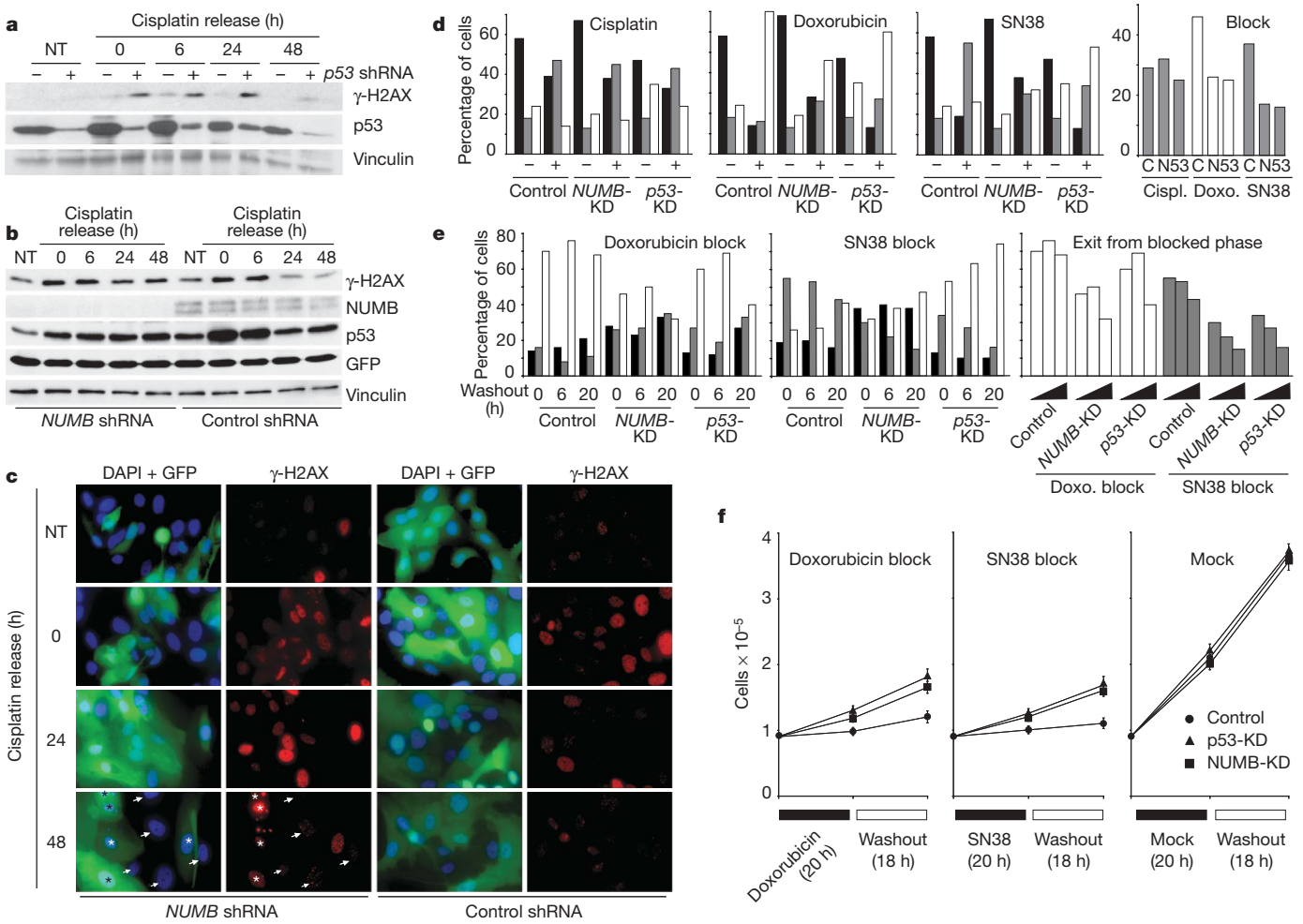

Figure 3 | *NUMB* silencing alters the p53-mediated response to DNA damage. **a**, **b**, MCF10A cells, in which *p53* (*p53* shRNA, **a**) or *NUMB* (*NUMB* shRNA, **b**) had been silenced, were treated with cisplatin (6 μg ml^{-1} for 15 h) and released in cisplatin-free medium. Immunoblot was as indicated. NT, not treated. **c**, γ-H2AX (red) in MCF10A cells, infected and treated as in **b**. Green (GFP), transduced cells. Asterisks, GFP-positive cells with persistent γ-H2AX staining. Arrowheads, non-infected cells with loss of γ-H2AX staining. Blue, 4,6-diamidino-2-phenylindole (DAPI). Original magnification, ×40. **d**, MCF10A, silenced with *p53* shRNA (*p53*-KD), *NUMB* shRNA (*NUMB*-KD) or control shRNA (Control) were mock-treated (−) or treated (+) for 24 h (cisplatin, 9 μg ml^{-1}; doxorubicin, 0.05 μg ml^{-1}; SN38, 10 ng ml^{-1}). Bars: solid, G1; grey, S; empty, G2/M. In the far-right 'Block' graph, values of the blocked phases are reported (cisplatin and SN38, S; doxorubicin, G2/M) in *NUMB*-KD (N), *p53*-KD (53) or control (C) cells. Values are expressed after subtracting cells in the same phase under non-treated conditions. **e**, MCF10A cells, silenced and treated as in **d**, were released in drug-free medium (washout) for 6 or 20 h, followed by fluorescence-activated cell sorting. For the 'Exit from the blocked phase' graph, values of the blocked phases (doxorubicin, G2/M; SN38, S) are reported versus time of drug washout (0, 6 or 20 h, triangles). **f**, MCF10A cells, silenced as in **d**, were treated for 20 h and then released in drug-free medium for 18 h. Cells were counted at the indicated times. **d**–**f** are representative of at least three experiments in triplicates.

that other endocytic proteins control various aspects of p53-mediated functions: dynamin 2 induces p53-dependent apoptosis[26], and the clathrin heavy chain promotes p53-mediated transcription[27] (see also Supplementary Discussion).

Finally, because NUMB is involved in binary fate decisions[1], a relevant question is whether NUMB, HDM2 or p53 are involved in the homeostasis of mammary stem cells, and in its subversion in tumours. The role of p53 in stem cells has been widely investigated, mostly in light of the induction of cellular senescence by p53, which in turn can be linked to the depletion of stem cells and to organism ageing[28]. Our data raise the possibility that p53, because of the NUMB liaison, is involved in the initial process that sits at the heart of stem cell fate (that is, asymmetric cell division). Indeed, a role for p53 as a cell-autonomous asymmetric kinetics control gene has been proposed[29], which might be due to its involvement in regulating the linked phenomenon of immortal DNA strand cosegregation[30]. Thus, our data put forward the possibility that an additional mechanism of tumorigenesis, caused by the lack of the p53/NUMB axis, is the skewing of stem cell division towards a symmetric pattern.

METHODS SUMMARY

Cultivation of primary epithelial cells was performed as described previously[5]. Procedures for immunofluorescence, immunoblotting and immunoprecipitation were also performed as described previously[5]. A list of the antibodies and reagents used is in Supplementary Information.

pG13–Luc and expression vectors for *p53* and *HDM2* were a gift of K. Helin. *p53* shRNA pSUPER was extracted from a shRNA library (a gift from R. Bernard). The retroviral PINCO–NUMB–GFP vector was as described[5]. The lentiviral pLL3.7 vector was a gift from L. Van Parijs. All constructs used in this study were sequence-verified. Procedures for retroviral infection and luciferase assays were also described[5]. Procedures for lentiviral infection are shown at http://web.mit.edu/ccr/labs/jacks/protocols/pll37.htm.

Specific siRNA for *NUMB* and controls were as described previously[5]. *NUMBL*- and *HDM2*-specific siRNA were from Dharmacon: *HDM2*, 5′-GCCACAAAUCUGAUAGUAU-3′; *NUMBL*, 5′-ACGCCUUCUGCUCAGC-CGC-3′.

Real-time PCR for *p53*, *HDM2*, *p21* (also known as *CDKN1A*), *p53R2* (also known as *RRM2B*), *PUMA* (also known as *BBC3*) and *FAS* was performed using the TaqMan Gene Expression Assays Indentification: Hs00153349-m1, Hs00242813-m1, Hs00355782-m1, Hs00153085_m1, Hs00248075_m1 and Hs00163653_m1, respectively (Applied Biosystems).

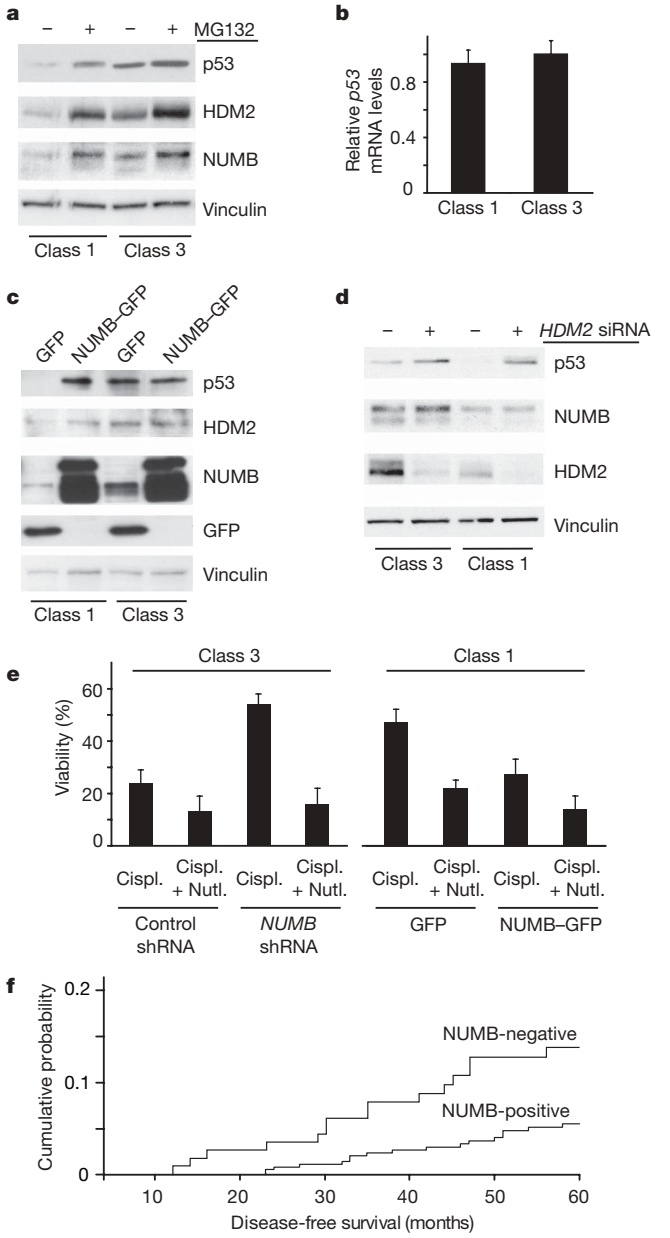

Figure 4 | Loss of NUMB in human breast tumours determines decreased p53, enhanced chemoresistance and predicts poor prognosis. a, Class 1 and class 3 cells were treated with MG132 (+). Immunoblot was as indicated. **b**, *p53* transcripts. Results represent mean (normalized to class 3) ± s.d. from four tumours. **c**, Class 1 and class 3 cells were transduced as shown. Immunoblot was as indicated. **d**, Class 1 and class 3 cells were transfected with *HDM2* siRNA (+) or control siRNA (−). Immunoblot was as indicated. **e**, Class 1 and class 3 cells were transduced as indicated, treated with cisplatin and nutlin, and analysed for cell viability. Results represent mean ± s.d. from triplicate points. In **a**, **c**, **d** and **e**, results are representative of four class 1 and four class 3 cultures, from different patients. **f**, NUMB status (as evaluated by immunohistochemistry) and prognosis (as evaluated by cumulative probability of any secondary event) in patients with breast cancer. Kaplan–Meier curves were compared by the Log-rank test. Hazard ratio before adjustment for clinical and pathological features (Cox proportional hazard method), 0.610 (*P*, 0.0068); hazard ratio after adjustment, 0.651 (*P*, 0.0291); Log-rank, 0.00387.

Full Methods and any associated references are available in the online version of the paper at www.nature.com/nature.

Received 1 March; accepted 23 October 2007.

1. Roegiers, F. & Jan, Y. N. Asymmetric cell division. *Curr. Opin. Cell Biol.* **16,** 195–205 (2004).
2. Santolini, E. *et al.* Numb is an endocytic protein. *J. Cell Biol.* **151,** 1345–1352 (2000).
3. Berdnik, D., Torok, T., Gonzalez-Gaitan, M. & Knoblich, J. A. The endocytic protein α-adaptin is required for numb-mediated asymmetric cell division in *Drosophila*. *Dev. Cell* **3,** 221–231 (2002).
4. Hutterer, A. & Knoblich, J. A. Numb and α-adaptin regulate Sanpodo endocytosis to specify cell fate in *Drosophila* external sensory organs. *EMBO Rep.* **6,** 836–842 (2005).
5. Pece, S. *et al.* Loss of negative regulation by Numb over Notch is relevant to human breast carcinogenesis. *J. Cell Biol.* **167,** 215–221 (2004).
6. Vousden, K. H. & Prives, C. p53 and prognosis: new insights and further complexity. *Cell* **120,** 7–10 (2005).
7. Hollstein, M., Sidransky, D., Vogelstein, B. & Harris, C. C. p53 mutations in human cancers. *Science* **253,** 49–53 (1991).
8. Momand, J., Zambetti, G. P., Olson, D. C., George, D. & Levine, A. J. The mdm-2 oncogene product forms a complex with the p53 protein and inhibits p53-mediated transactivation. *Cell* **69,** 1237–1245 (1992).
9. Haupt, Y., Maya, R., Kazaz, A. & Oren, M. Mdm2 promotes the rapid degradation of p53. *Nature* **387,** 296–299 (1997).
10. Kubbutat, M. H., Jones, S. N. & Vousden, K. H. Regulation of p53 stability by Mdm2. *Nature* **387,** 299–303 (1997).
11. Zhang, Y., Xiong, Y. & Yarbrough, W. G. ARF promotes MDM2 degradation and stabilizes p53: ARF-INK4a locus deletion impairs both the Rb and p53 tumor suppression pathways. *Cell* **92,** 725–734 (1998).
12. Oliner, J. D., Kinzler, K. W., Meltzer, P. S., George, D. L. & Vogelstein, B. Amplification of a gene encoding a p53-associated protein in human sarcomas. *Nature* **358,** 80–83 (1992).
13. Sherr, C. J. Tumor surveillance via the ARF–p53 pathway. *Genes Dev.* **12,** 2984–2991 (1998).
14. McCann, A. H. *et al.* Amplification of the *MDM2* gene in human breast cancer and its association with MDM2 and p53 protein status. *Br. J. Cancer* **71,** 981–985 (1995).
15. Pharoah, P. D., Day, N. E. & Caldas, C. Somatic mutations in the p53 gene and prognosis in breast cancer: a meta-analysis. *Br. J. Cancer* **80,** 1968–1973 (1999).
16. Vestey, S. B. *et al.* $p14^{ARF}$ expression in invasive breast cancers and ductal carcinoma *in situ*—relationships to p53 and Hdm2. *Breast Cancer Res.* **6,** R571–R585 (2004).
17. Sharpless, N. E. & DePinho, R. A. The INK4A/ARF locus and its two gene products. *Curr. Opin. Genet. Dev.* **9,** 22–30 (1999).
18. Silva, J. *et al.* Analysis of genetic and epigenetic processes that influence $p14^{ARF}$ expression in breast cancer. *Oncogene* **20,** 4586–4590 (2001).
19. Silva, J. *et al.* Concomitant expression of *p16INK4a* and *p14ARF* in primary breast cancer and analysis of inactivation mechanisms. *J. Pathol.* **199,** 289–297 (2003).
20. Juven-Gershon, T. *et al.* The Mdm2 oncoprotein interacts with the cell fate regulator Numb. *Mol. Cell. Biol.* **18,** 3974–3982 (1998).
21. Vassilev, L. T. *et al. In vivo* activation of the p53 pathway by small-molecule antagonists of MDM2. *Science* **303,** 844–848 (2004).
22. Rogakou, E. P., Pilch, D. R., Orr, A. H., Ivanova, V. S. & Bonner, W. M. DNA double-stranded breaks induce histone H2AX phosphorylation on serine 139. *J. Biol. Chem.* **273,** 5858–5868 (1998).
23. Paull, T. T. *et al.* A critical role for histone H2AX in recruitment of repair factors to nuclear foci after DNA damage. *Curr. Biol.* **10,** 886–895 (2000).
24. Reis, T. & Edgar, B. A. Negative regulation of dE2F1 by cyclin-dependent kinases controls cell cycle timing. *Cell* **117,** 253–264 (2004).
25. Lowe, S. W., Ruley, H. E., Jacks, T. & Housman, D. E. p53-dependent apoptosis modulates the cytotoxicity of anticancer agents. *Cell* **74,** 957–967 (1993).
26. Fish, K. N., Schmid, S. L. & Damke, H. Evidence that dynamin-2 functions as a signal-transducing GTPase. *J. Cell Biol.* **150,** 145–154 (2000).
27. Enari, M., Ohmori, K., Kitabayashi, I. & Taya, Y. Requirement of clathrin heavy chain for p53-mediated transcription. *Genes Dev.* **20,** 1087–1099 (2006).
28. Sharpless, N. E. & DePinho, R. A. Telomeres, stem cells, senescence, and cancer. *J. Clin. Invest.* **113,** 160–168 (2004).
29. Sherley, J. L., Stadler, P. B. & Johnson, D. R. Expression of the wild-type p53 antioncogene induces guanine nucleotide-dependent stem cell division kinetics. *Proc. Natl Acad. Sci. USA* **92,** 136–140 (1995).
30. Rambhatla, L., Ram-Mohan, S., Cheng, J. J. & Sherley, J. L. Immortal DNA strand cosegregation requires p53/IMPDH-dependent asymmetric self-renewal associated with adult stem cells. *Cancer Res.* **65,** 3155–3161 (2005).

Supplementary Information is linked to the online version of the paper at www.nature.com/nature.

Acknowledgements We thank K. Helin for the p53 and HDM2 reagents; L. Van Parijis for the pLL3.7 lentiviral vector; R. Bernard for the *p53* shRNA pSUPER vector; G. Matera for technical assistance; P. Maisonneuve and G. Goisis for statistical analysis; the Imaging Service at IEO; and the Real Time PCR Service at IFOM. This work was supported by grants from the Associazione Italiana per la Ricerca sul Cancro and MIUR to S.P. and P.P.D.F., from the European Community (VI Framework), The Ferrari Foundation, the Monzino Foundation and the CARIPLO Foundation to P.P.D.F., and from the G. Vollaro Foundation to S.P.

Author Contributions I.N.C., D.T., F.S.-N. and S.P. performed experimental work. P.N., V.G. and G.V. performed the clinical part of the work (patient selection, histology and data analysis of the patient's case collection). S.P. and P.P.D.F. planned and supervised the project, performed data analysis and wrote the manuscript.

Author Information Reprints and permissions information is available at www.nature.com/reprints. Correspondence and requests for materials should be addressed to S.P. (salvatore.pece@ifom-ieo-campus.it) or P.P.D.F (pierpaolo.difiore@ifom-ieo-campus.it).

METHODS

Cells and reagents. Cultivation of primary normal and tumour human mammary epithelial cells was as described previously[5]. These cells can be cultivated from tumours displaying low or absent levels of NUMB (class 1) or from tumours showing normal levels of NUMB (class 3). Primary cultures are used within 7–10 days from explant to prevent adaptation to the cell culture conditions, and constitute, therefore, a rather faithful representation of the parenchymal component of breast tumours[5].

For survival assays (Fig. 4e), primary tumour cells were plated in six-well plates. Subconfluent cells were treated with cisplatin (12 μg ml^{-1}) for 15 h and then grown in cisplatin-free medium (plus or minus nutlin) for 96 h. Cells were then stained with 0.05% crystal violet for 10 min and then extensively rinsed with water. The crystal violet retained by live cells was leached in acetic acid (10%) and absorbance was read at 595 nm.

Antibodies were: anti-Flag M2-agarose Affinity Gel from Sigma; anti-p53 (DO-1 and FL-393), anti-NOTCH1 (c-20), anti-HDM2 (SMP14) and anti-PUMA (N-19) from Santacruz Biotechnology; anti-phospho-p53–Ser 15 and anti-cleaved caspase-3 (Asp 175) from Cell Signaling; anti-ubiquitin (FK2, BioMol); anti-phospho-histone H2AX (Ser 139) from Upstate; and anti-NUMB monoclonal antibody (Ab21, generated against amino acids 537–551 of human NUMB). Fluorochrome-conjugated secondary antibodies were from Jackson ImmunoResearch Laboratories. MG132 (Affinity) was used at 10 μM. The GSIs DAPT (*N*-[*N*-(3,5-difluorophenacetyl)-L-alanyl]-*S*-phenylglycine *t*-butyl ester), and DFP-AA (*N*-[*N*-(3,5-difluorophenacetyl)]-L-alanyl-3-amino-1-methyl-5phenyl-1,3-dihydro-benzo[e](1,4)diazepin-2-one) (Calbiochem) were used at 1 μM. Nutlin-3 (Cayman) was used at 8 μM. In the experiments shown in Fig. 1b, Nutlin was used at 20 μM.

Cell cycle analysis. Cells were washed with PBS and were subsequently fixed in 70% ethanol and either stored at 4 °C or directly used for staining with propidium iodide. For propidium iodide staining, cells were washed once in PBS supplemented with 1% BSA and were counterstained overnight with 5 μg ml^{-1} propidium iodide and 40 μg ml^{-1} RNase. The samples were analysed with a Becton Dickinson FACScan.

Engineering of vectors, siRNA experiments, and quantitative PCR. pG13–Luc, a luciferase reporter controlled by multimeric p53 binding sites, and expression vectors for *p53* and *HDM2* were a gift from K. Helin. A retroviral vector to silence *p53* (*p53*-shRNA pSUPER) was extracted from a shRNA library (a gift from R. Bernard). The retroviral PINCO–NUMB–GFP vector was as described[5]. The lentiviral pLL3.7 vector (a gift from L. Van Parijs) was used to clone sh-RNAs under the control of the mouse U6 promoter, upstream of a CMV–GFP expression cassette[31]. Target sequences were: 5′-GGTTAAGTACCTTGGCCATGT-3′ and 5′-AGACGAACAAGTCACCGACTT-3′ for *NUMB* and control, respectively. Constructs harbouring *GST–NUMB*, *hNΔE* and *hNICD* (which represent two different gain-of-function mutants of the NOTCH1 receptor, see Supplementary Fig. 4) were engineered by PCR starting from a pcDNAIII FL-NUMB or pcDNAIII FL-NOTCH1 plasmid. All constructs were sequence-verified. Details are available on request. Procedures for retroviral infection and luciferase assays were also described[5]. Procedures for lentiviral infection are at http://web.mit.edu/ccr/labs/jacks/protocols/pll37.htm.

Specific siRNAs for *NUMB* and the corresponding control were described previously[5]. *NUMBL*- and *HDM2*-specific siRNA were obtained from Dharmacon: *HDM2*, 5′-GCCACAAAUCUGAUAGUAU-3′; *NUMBL*, 5′-ACGCCUUCUGCUCAGCCGC-3′. Cells were transfected using Oligofectamine (Invitrogen) for 72 h (siRNA concentration, 100 nM). For double *NUMB* and *HDM2* ablation, MCF10A cells were infected with *NUMB* shRNA (or control shRNA) for 120 h and were then transfected with *HDM2* siRNA (or control siRNA) oligonucleotides for 48 h.

The relative quantity of mRNA transcripts for p53, HDM2, p21, p53R2, PUMA and FAS was determined by real-time PCR with TaqMan Gene Expression Assays Identification: Hs00153349-m1, Hs00242813-m1, Hs00355782-m1, Hs00153085_m1, Hs00248075_m1 and Hs00163653_m1, respectively (Applied Biosystems).

Biochemical studies. Procedures for immunofluorescence, immunoblotting and immunoprecipitation were also performed as described[5].

For the binding assays in Fig. 1b (and in Supplementary Fig. 1b), NUMB, p53 and HDM2 were bacterially expressed as GST-fusion proteins. GST fusions harbouring NUMB and HDM2 were cleaved and purified with the Thrombin Cleavage Capture Kit (Novagen). p53–GST was not cleaved, and was used as such. Purified proteins were incubated for 6 h at 4 °C in 300 μl of binding buffer (25 mM Tris-Cl, pH 7.2, 50 mM NaCl and 0.2% Nonidet P-40) with continuous shaking. Recovery of proteins was achieved (4 h at 4 °C) with either glutathione agarose beads (Pharmacia; for p53–GST pulldown) or protein G beads (Zymed) preconjugated to NUMB (AB21) or HDM2 (SMP14, Santa Cruz) antibody (for NUMB or HDM2 immunoprecipitation, respectively). Beads were washed three times with a large excess of washing buffer (100 mM Tris-Cl, pH 8.0, 100 mM NaCl and 1% Nonidet P-40), and were boiled in protein sample buffer. Eluted proteins were resolved by SDS–PAGE.

For the *in vitro* ubiquitination assay in Fig. 2g, NUMB, p53 and HDM2 were bacterially expressed as GST-fusion proteins. GST fusions harbouring NUMB and HDM2 were cleaved and purified with the Thrombin Cleavage Capture Kit (Novagen). Assays were performed as described[32]. In brief, reaction mixtures contained purified enzymes (150 ng E1 (a ubiquitin-activating enzyme), 150 ng purified His-tagged UbcH5B and 0.4 μg HDM2), 2.0 μg of GST–p53 fusion and 5 μg of ubiquitin in ubiquitination buffer (25 mM Tris-HCl, pH 7.6, 5 mM $MgCl_2$, 100 mM NaCl, 1 mM DTT, 2 mM ATP). When appropriate, 2.0 μg NUMB were added to the reaction mixture. Reactions were incubated at 30 °C for 1 h, followed by four washes in 1% Triton/0.1% SDS buffer, and were subjected to detection in immunoblot.

For sequential immunoprecipitations, total cellular lysates from HEK293 cells overexpressing HDM2, Flag–NUMB and p53 (Supplementary Fig. 1c), or total cellular lysates from U2OS (Fig. 1c, endogenous proteins), were used. After the first immunoprecipitation step using an anti-Flag M2 affinity resin (for the overexpressed Flag–NUMB, Supplementary Fig. 1c) or anti-NUMB (AB21) antibody (for the endogenous protein, Fig. 1c), immunoprecipitates were eluted with the Flag peptide (Sigma) or with the immunogenic NUMB peptide (amino acids 537–551) (Eurogentec), and were then further immunoprecipitated and immunoblotted as described in the legends to the Figures. That panels shown in Fig. 1c were assembled from different lanes of the same blots by splicing out lanes loaded with additional controls.

Experiments with inhibitors of presenilin/γ-secretase. The GSI DFP-AA (also known as Compound E) and DAPT (Calbiochem) were used at 1 μM in the experiments shown in Fig. 2h and Supplementary Fig. 4a. These compounds are benzodiazepine-type compounds that act as highly potent, selective and non-competitive inhibitors of γ-secretase/presenilin by binding the active site of presenilin-1 and presenilin-2. This enzymatic activity is critical for the physiological activation of NOTCH, because it executes the cleavage of the NOTCH receptor at the so-called S3 site (located at the end of the transmembrane region) to release the NOTCH intracytoplasmic tail; this then translocates to the nucleus and executes NOTCH function.

Selection of breast cancer patients and statistical analysis. To establish a possible correlation between NUMB status of breast tumours and patient outcome, we used data from 443 breast cancer patients enrolled in a surgical trial[33] conducted at the European Institute of Oncology between March 1998 and December 1999. Immunohistochemical analysis of NUMB was performed by tissue microarray, as described[5]. In brief, breast tumours displaying NUMB expression in less than 10% of tumour cells were scored as NUMB-negative (114 patients), whereas tumours showing more than 10% NUMB-expressing cells were scored as NUMB-positive (329 patients).

The 443 patients were followed for a median of 54.8 months (range 4.3–60). During the follow-up period, a total of 40 new events were registered. Ten patients developed a loco-regional event, 9 developed a controlateral carcinoma, and 21 developed a distant metastasis. Association between the clinical/pathological features of the tumours and NUMB expression was evaluated by the Pearson chi-squared test (see Supplementary Table 1). Plots of the cumulative incidence of events according to NUMB expression were drawn using the Kaplan–Meier method and compared by the Log-rank test (see Fig. 4f). Univariate and multivariate analysis was carried out by means of the Cox proportional hazards method to assess the prognostic value of NUMB status before and after correction for well-recognized prognostic factors, including age at diagnosis of the tumour, pathological stage, tumour grade of differentiation, hormone-receptor status, nodal status, Ki-67 and HER-2/neu expression. SAS statistical software was used for all the analysis (SAS Institute, Inc.). A P value of less than 0.05 was considered as significant.

31. Rubinson, D. A. *et al.* A lentivirus-based system to functionally silence genes in primary mammalian cells, stem cells and transgenic mice by RNA interference. *Nature Genet.* **33**, 401–406 (2003).
32. Woelk, T. *et al.* Molecular mechanisms of coupled monoubiquitination. *Nature Cell Biol.* **8**, 1246–1254 (2006).
33. Veronesi, U. *et al.* A randomized comparison of sentinel-node biopsy with routine axillary dissection in breast cancer. *N. Engl. J. Med.* **349**, 546–553 (2003).